GEOMAGNETIC CONTROL ON THE EQUATORIAL PLASMA BUBBLE FORMATION

© 2025 L. N. Sidorova

Pushkov Institute of Terrestrial Magnetism, Ionosphere and Radiowave Propagation (IZMIRAN), Moscow, Troitsk, Russia

e-mail: lsid@izmiran.ru

Received May 01, 2024

Revised June 15, 2024

Accepted July 25, 2024

Abstract. Attempts have been made repeatedly to investigate the effect of magnetic activity on the equatorial plasma bubble (EPB) generation. At the moment, it is generally accepted that magnetic activity tends to suppress the EPB generation and evolution in the pre-midnight sector. As for the post-midnight sector, it is believed that the EPB occurrence probability will increase after midnight as magnetic activity increases. Moreover, the growth rates of the EPB occurrence probability will strongly depend on solar activity: at the solar activity minimum, they will be the most significant. A sufficient amount of the observations is required to confirm these ideas. For this purpose, the EPB observations obtained on board the ISS-b satellite (~972−1220 km, 1978−1979) in the pre- and post-midnight sectors are best suited. The data were considered in two latitudinal regions: equatorial/low-latitudinal (±20°) and mid-latitudinal ±(20°−52°) regions. LT- and *Kr*-variations of the EPB occurrence probability were calculated for both groups. (1) It was revealed that the occurrence probability maximum of the EPBs recorded at the equator and in low latitudes is in the pre-midnight sector. The EPB occurrence probability decreases with increasing *Kr* index with a delay of 3 and 9 hours before the EPB detection. (2) However, the occurrence probability maximum of the EPBs recorded at the mid-latitudes is in the post-midnight sector. Their occurrence probability increases slightly as *Kr* index increases, when *Kr* is a 9-hours delayed one. Thus, the idea of the ionospheric disturbance dynamo (IDD) influence on the post-midnight EPB generation has been confirmed. IDD mechanism sets in after some hours of enhanced geomagnetic activity and favors the generation. However, its influence is weakened during the years of increased solar activity.

DOI: 10.31857/S00167940250608e3

1. INTRODUCTION

Since the pioneering work of Woodman and La Hoz [1976], it has been generally accepted that equatorial plasma bubbles (EPB) or equatorial spread F (ESF) are formed after sunset under the influence of the Rayleigh-Taylor (RT) plasma instability that develops at the base altitudes of the *F* region. Namely, in the evening period, when the solar terminator crosses equatorial latitudes, a sharp burst of eastward electric fields (pre-reversal enhancement, PRE) is observed. The burst of fields causes a powerful upward E × B drift, which leads to a rapid rise of the base of the equatorial *F*-region to heights where the rate of growth of the RT unsteadiness dominates and becomes decisive. As a result, favorable conditions for the generation of the ERV (ESF) arise

In addition to diurnal variability, the equatorial electric fields experience perturbations during geomagnetic storms under the influence of two high-latitude factors - magnetic perturbations arising from the effect of the solar wind on the Earth's magnetosphere [Senior and Blanc, 1984], and ionospheric perturbations [Blanc and Richmond, 1980].

Dynamic interactions between the solar wind and the magnetosphere, leading to changes in the potential in the polar cap, cause the appearance of so-called prompt penetration electric fields (PP) at low latitudes and lead to an increase in the perturbation of zonal electric fields [Kelley et al., 1979; Fejer and Scherliess, 1997]. The prompt penetration electric fields (PP) are short-lived (~ 1− 2 h) and propagate almost instantaneously to low and equatorial latitudes [Fejer, 1991].

The ionospheric disturbances appear due to the development of the global thermospheric circulation induced by Joule heating at auroral latitudes. As the circulation processes develop, the ionospheric disturbance dynamo (IDD) generates long-lived electric field perturbations at middle and low latitudes [Scherliess and Fejer, 1997]. At equatorial latitudes, IDDs cause the appearance of long-lived (several hours) electric fields with a westerly direction in the pre-midnight sector. These processes develop rather slowly − several hours from the onset of a geomagnetic storm (substorm) [Fejer and Scherliess, 1995]. According to Blanc and Richmond [1980], the time delay between the onset of a substorm and the development of a strong electric field at equatorial latitudes can reach ~9 h).

As a result, the superposition of electric fields of different nature (PP and IDD) can either strengthen or weaken the PRE effect during sunset. In other words, the electric fields of PP and wind dynamo fields (IDD), superimposed on the regular variations of the equatorial electric fields, can either favor the processes of PRE generation or suppress them. The growth/suppression of EPWs is believed to depend on the relative contributions of PP and IDD fields as a function of storm onset and local time [Martinis et al., 2005; Basu et al., 2007]. For example, as shown by Martinis et al. [2005], there is a robust relationship between the post-occupation EPW and rapid temporal changes in the interplanetary electric field caused by variations in the *Bz* component of the IMF. These changes

contribute to the instantaneous development of PP fields of easterly polarity, which is a favorable situation for the growth of RT instability. On the other hand, the IDD mechanism at equatorial latitudes causes the emergence of long-lived electric fields having a westerly direction in the pre-midnight sector, which leads to the suppression of the RT-unsteadiness rates. These long-lived fields, initiated, for example, by a number of successive substorms, have a property to overlap and create a long-lasting effect of suppression of the EWR generation.

As a result, a rather complicated and confusing picture of the influence of geomagnetic activity (influence through different mediators) on the processes of ESF generation emerges.

Attempts to study this influence have been repeatedly made. At present, the researchers have come to a consensus that geomagnetic activity tends to suppress ESF generation in the pre-midnight sector. (In other words, as the *Kr*-index increases, there is a decrease in the probability of observing ESF.) As for the postmidnight sector, it is believed (see, for example, [Bowman, 1978; Burke, 1979; Singh et al., 1997]) that the probability of observing ESF after midnight will increase as the geomagnetic activity increases.

To achieve a better understanding of the relative contribution of different mediators (PP and IDD) to the energy transfer of geomagnetic storms, studies related to the study of the delay of the influence of the *Kr*-index as an indicator of storm activity on the generation/development of ERW were carried out (see, for example, [Palmroth et al., 2000; Sobral et al., 2002; Li et al., 2009]). Obviously, taking into account the delay of the *Kr*-index allows one to "cut off" the instantaneous influence of short-lived electric PP fields with some probability. It was found [Li et al., 2009] that magnetic activity confidently suppresses the generation of EPW with a time delay of 4-9 hours in the equatorial region and with a delay of 8-9 hours in the low-latitude region. Only pre-midnight EPWs were considered (the post-midnight ones were insufficient for statistical analysis). In [Sobral et al., 2002], using data for 22 years of optical observations, it was found that for changes in the *Kr-index* in the period 18-21 LT (i.e., at the start of EPW development), the probability of observing EPWs first decreased as the Kr-index increased up to 5, and, on the contrary, increased with $Kr \geq 5$. Unfortunately, the authors did not specify the sector of ERV observations. However, other researchers [Palmroth et al., 2000], based on data from the DE 2 satellite, made a clear division of EPWs into observation sectors. For the evening cases (19-23 MLT), it was found that the best inverse correlation occurred when the *Kr*-index was delayed by 2 and 9 hours. For the morning cases (23-06 MLT), a direct correlation was found, with the best correlation occurring with a *Kr*-index delay of 2-4 hours and 9 hours.

In the present work, we continued to study the delayed effect of the *Kr*-index on the development of EPB throughout the night. Special attention is paid to the post-midnight sector. It is important to note that this study was possible due to the fact that significant material has been

accumulated (ISS-b satellite data) concerning EPW cases registered at upper ionospheric heights (~1000 km) in both the pre-midnight and post-midnight sectors [Sidorova, 2020; 2021; 2022]. Using ISS-b satellite data, histograms of the probability of ERW observations were calculated as a function of latitude, local time, month of the year, etc., which allowed us to obtain a clear spatial and temporal picture of the ERW evolution at upper ionospheric heights [Sidorova, 2020; 2021; 2022; 2023a, b]. These results were extremely useful and facilitated the present study.

To fulfill this task, we calculated the histograms of the probability of EPB observations depending on the local time (LT) and the level of geomagnetic activity (*Kr*). The EPBs were divided into two groups by the latitudinal characteristic of observations: equatorial-low-latitude and middle-latitude EPBs. The dependence of the probability of observing different groups of EPBs on the level of geomagnetic activity (*Kr*) was investigated for three cases when the *Kr*-index delay was 3, 6, and 9 hours.

2. COMPARATIVE ANALYSIS DATA

The histograms of EPB occurrence probability (EPB occurrence probability, P_{EPB}) as a function of local time (LT) and the level of geomagnetic activity (*Kr*) were calculated using data from the ISS-b satellite [RRL, 1983; 1985]. The ISS-b satellite flew during years of high solar activity (*F10*.7~150-220, 1978-1979), had a quasi-circular orbit with an inclination of ~70°, covering the altitudes of the upper ionosphere (~972− 1220 km). Observations aboard the satellite were conducted for 17 months (August 1978− December 1979) [RRL, 1983; 1985].

Observations of plasma regions with reduced He^+ concentration were used to construct histograms. According to [Sidorova and Filippov, 2012; Sidorova and Filippov, 2013], these regions registered at the heights of the upper ionosphere can be interpreted as plasma bubbles of equatorial origin (EPB). Only those EPBs (He^+ depleted regions) whose concentration decreased by a factor of one and a half or more with respect to the background were used for the construction.

2.1 Variations of P_{EPB} as a function of local time (LT)

To construct the LT-variations of P_{EPB} the data on EPB observations in the 17-08 LT interval were used. The EPB cases were considered independently of the level of geomagnetic activity, i.e. at all values of the *Kr*-index. The P_{EPB} values were calculated as median values for two latitudinal regions covering both hemispheres. The equatorial and low latitude region ±20° (Fig. 1*a*) was considered, as well as the predominantly mid-latitude region ± (20°–52°) (Fig. 1*b*), which overlapped the low latitudes in the interval ±(20°-23.3°). (The accuracy of fixing the orbital parameters of the ISS-b satellite given in the catalogs [RRL, 1983; 1985] is low, so the ±20° boundary is rather tentative.

Further, for ease of narration, we will refer to this region as ″mid-latitude″). The choice of the indicated latitude regions is related to the following.

Fig. 1.

When the bubble rises to the upper ionospheric heights (ISS-b, ~972-1220 km) under the influence of ambipolar diffusion, the bubble "spreads" along the magnetic force tubes. As a result, the bubble acquires a banana-shaped appearance. In this form, the bubble can be registered not only in equatorial and low latitudes, but also at middle latitudes. The figure clearly shows that the middle (apex) part of the rising bubble is registered above the equator, and its ends are registered at low or middle latitudes. The picture of the bubble structure development was confirmed in studies of latitudinal distributions of P_{EPB} conducted at different altitudes [Sidorova, 2021]. It was found that with increasing altitude, additional midlatitudinal probability maxima develop in latitudinal distributions of P_{EPB} in addition to the central (equatorial) probability maximum. The growth and development of the midlatitudinal maxima is explained by the fact that the ERV has reached its ceiling heights. (A bubble that has lost the ability for further ascent experiences deceleration, stops at the power tube corresponding to the ceiling height, and after a few hours experiences compression (collapse). Such bubbles, frozen at their ceiling heights, accumulate, which is reflected in the appearance of mid-latitude maxima of P_{EPB} at the heights of the upper ionosphere).

In view of the above, the choice of latitudinal areas of EPW study was determined by the latitudes of the development of these maxima, i.e., the areas of preferential registration of EPW.

2.2 Variations of P_{EPB} depending on the level of geomagnetic activity (Kr)

To construct the *Kr*-variation of *P*(EPB), data on EPB observations at different intervals of the *Kr*-index variation were used. We considered 5 intervals of the *Kr*-index reflecting calm, moderately perturbed and perturbed geomagnetic conditions: (0–1), (1^+–2), (2^+–3), (3^+–4), (4^+–9). Since strong and very strong geomagnetic disturbances of different intensities did not occur very often, they were combined into one interval to improve the statistical sampling: the *Kr*-index varied from 4^+ to 9.

P_{ERV} values were calculated as median values for two latitudinal regions covering both hemispheres. The equatorial and low latitude region ±20° (Fig. 2) and the mid-latitude region ±(20°–52°) (Fig. 3) were considered.

Fig. 2.

Fig. 3.

Three delayed cases were considered to study the effect of delaying the influence of the *Kr*-index, as an indicator of storm activity, on ERW generation. In the first case (Figs. 2*a*, 3*a*), *Kr*-index values taken 3 hours before ERW registration were used. In the second case (Fig. 2*b*, 3*b*) - 6 hours

before ERV registration. In the third case (Fig. 2*c*, 3*c*), respectively, 9 hours before EPO registration. The numerical characteristics of the mentioned variations are reflected in Tables 1, 2.

Table 1.

Table 2.

3. COMPARATIVE ANALYSIS

1. We perform a detailed comparative analysis of the LT variations of the EPB observation probability (P_{EPB}) detected in different latitude regions (Fig. 1*a*, *b*).

The LT variations of P_{EPB} obtained at the equator and at low latitudes ±20° have a maximum probability occurring at ~20:00-23:00 LT, i.e., in the pre-midnight sector. By midnight, the P_{EPB} values experience a drop and remain at approximately the same rather high level for the entire post-midnight period up to ~05:00 LT. On the other hand, the LT variations of P_{EPB} obtained at mid-latitudes ±(20°-52°) have a maximum at post-midnight (~02:00-04:00 LT). The P_{EPB} values increase smoothly after sunset until the specified period, and then experience a sharp drop by the sunrise hour.

2. Let us now turn to the *Kr*-variations of P_{EPB} (Figs. 2, 3).

The *Kr*-variations of P_{EPB} obtained at the equator and low latitudes ±20° (Fig. 2) show a weak inverse dependence of P_{EPB} on *Kr* when the *Kr*-index is delayed by 3 hours. When the *Kr*-index is delayed by 6 h, this dependence is broken. However, when *Kr*-index is delayed by 9 hours, it recovers and becomes significant: with increasing *Kr*, P_{EPV} values clearly decrease.

The *Kr*-variations of P_{EPB} obtained in the midlatitude region ±(20°-52°) (Fig. 3), at *Kr*-index delays of 3− 6 hours, do not have a clear dependence of P_{EPB} on *Kr*. However, at *Kr*-index delays of 9 hours, P_{ERV} values are in direct dependence on Kr-index: they increase slightly with increasing *Kr* values.

It should be pointed out that the Kr-variations *of* P_{ERV} in the equatorial-low-latitude region vary between 24-41%, and in the mid-latitude region between 56-64%. Indeed, as the histograms and Tables 1, 2 show, the amount of mid-latitude EPWs clearly prevails over equatorial-low latitude EPWs.

4. DISCUSSION

1. As stated in the Introduction, the main goal of the current study is to investigate the influence of geomagnetic activity on the EPW generation. However, in order to understand the details of this influence, it is necessary to have a picture of the EPW evolution, for example, in the latitude-time sweep. The ISS-b satellite data allowed us to obtain this picture at fixed heights of the upper ionosphere. From these data, LT variations of P_{ERV} were obtained in different latitudinal regions.Let us discuss them.

It was found that ERVs recorded at the equator and at low latitudes ±20° dominate (have maximum observational probability) in the pre-midnight sector. On the other hand, ERVs registered at mid-latitudes ±(20°–52°) dominate in the post-midnight sector. It is reasonable to wonder about the causes of this phenomenon.

Previously (see, e.g., [Sidorova, 2020]), it was revealed from a number of satellite data (CHAMP, AE-E, ROCSAT-1, Hinotori, ISS-b) that with increasing observation altitude there is a clear tendency for the maximum of the ERV observation probability to shift in time. Thus, while at the base altitudes of the *F*-region the maximum occurs in the post-sunset hours (~20:30– 22:00 LT, CHAMP, AE-E, ~400 km), as the observation altitude increases, it shifts to the pre-midnight hours (~21:00– 24:00 LT, ROCSAT-1, ~600 km), then to post-midnight (~01:00– 03:00 LT, Hinotori, ~650 km) and finally to predawn (~03:00– 04:00 LT, ISS-b, ~972-1220 km) hours. To explain this phenomenon, we should refer to Fig. 4.

Fig. 4.

As already mentioned (see, for example, [Sidorova, 2021]), plasma bubbles, as they rise to higher heights under the influence of ambipolar diffusion, begin to "stretch/spread" along the magnetic force tubes, taking on a banana-shaped appearance (Fig. 4). In the initial phase of their development, the bubbles are registered strictly within the equatorial region, since they experience still extremely insignificant diffusion "spreading". As a result, the appearance ("arrival") of such EPBs is registered as a clear maximum probability in the pre-midnight sector [Stolle et al., 2006]. Further, as the bubbles rise, the diffusion "spreading" processes come into full force and EPWs can be registered not only in equatorial, but also in low latitudes. The maximum of their probability gradually "blurs": the top becomes flatter and the descent becomes more gentle and long [Watanabe and Oya, 1986; Li et al., 2009; Sidorova, 2020]. We obtained LT variations of P_{ERV} for ERV cases detected at the equator and at low latitudes ±20° (Fig. 1*a*). Obviously, at ISS-b altitudes (~972-1220 km), bubble tops or parts of bubbles closest to the tops are detected at these latitudes. At the same time, the maximum probability of the "arrival" of EPB still remains in the pre-midnight sector. Further rise of the bubble to the upper ionosphere heights leads to the fact that its "ends" begin to be projected to the middle latitudes. Most of the bubbles reach their ceiling heights, stop at them and accumulate. Their accumulation is reflected in the appearance of a predawn maximum on the histogram of the LT-distribution of the probability of EPB observations calculated over the entire latitude range ±50° [Sidorova, 2020]. And this predawn maximum (~ 04:00-03:00:00 LT) is most clearly manifested in the LT variations of P_{EPB}, calculated specifically for the midlatitude region ±(20°–52°) (Fig. 1*b*).

Notably, these variations are identical to the LT-variations of the probability of observing post-midnight ESF observations obtained in Fejer et al. [1999] (Fig. 12 of the above paper).

In view of the above, the binding to the latitudinal regions ±20° and ±(20°–52°) is due not only to the fact that they are the areas of preferential registration of EPV (as shown earlier in Section 2.1), but also to the fact that the features of LT variations of P_{EPV} are manifested there.

2. Let us now turn to the subject of the study, namely, let us discuss the variations of P_{EPW} plotted as a function of the level of geomagnetic activity (*Kr*) (Figs. 2, 3). Let us analyze the delay effect of the Kr-index influence on the EPW development in different sectors of observations.

a) Let us consider the EPWs detected in the ±20° region (equator and low latitudes) and dominating in the pre-midnight sector. It was obtained that their P_{ERV} variations are in a weak inverse dependence on *Kr* when the latter is delayed by 3 h (Fig. *2a*). This trend is broken when *Kr*-index is delayed by 6 hours (Fig. 2*b*) and is restored when *Kr*-index *is* delayed by 9 hours. Moreover, in the latter case, the inverse dependence becomes very pronounced (Fig. 2*c*).

It should be noted that the results obtained agree quite well with the results of studies obtained from the DE 2 satellite data (~309-1012 km, 1981-1983) [Palmroth et al., 2000]. There, the Kr-variations *of* P_{EPB} detected in the pre-midnight sector (19-23 MLT) showed an inverse dependence on the *Kr*-index when the latter was delayed by 2 hours. Then this dependence was broken and restored only when *Kr*-index was delayed by 9 hours (see Fig. 7 in [Palmroth et al., 2000]).

A similar trend was observed in the behavior of histograms P_{EPB} calculated for 3 years of observations from data of ground-based sounding stations at equatorial and low latitudes of Southeast Asia [Li et al., 2009]. Thus, at the equator, the inverse dependence appeared at a delay of the *Kr*-index by 4 hours, and at low latitudes - at a delay of the *Kr*-index by 8-9 hours (see Figs. 8-9 in [Li et al., 2009]).

Thus, our results do not contradict the previously known results. It is known that in the pre-midnight sector, the EPW generation is suppressed due to the development of long-lived perturbed electric fields of the western polarity developing several hours after the storm activity. These perturbed fields appear under the influence of the ionospheric wind dynamo or the so-called IDD effect (ionospheric disturbance dynamo, IDD) developing at middle and low latitudes a few hours after the onset of the storm [Scherliess and Fejer, 1997]. The perturbed electric fields are superimposed on the electric fields of the regular dynamo effect, which remains active even during the periods of geomagnetic disturbances. At the same time, the EPW generation does not stop at all, but is only suppressed as the growth rate of RT-unsteadiness decreases.

Obviously, the electric fields of rapid or direct penetration (PP) also have their influence. They can both favor the generation of ERV and suppress it. Their influence develops instantly,

however, it does not last long (~1− 2 h), so they practically do not affect the effect associated with the delay of Kr-index influence.

According to our results, the IDD effect starts to appear when Kr-index is delayed already for 3 hours, which agrees well with the indication of Fejer and Scherliess [1995]. Further the IDD effect is disrupted. However, it recovers when the Kr-index *is* delayed by 9 hours, which again agrees with the findings of Blanc and Richmond [1980].

b) Consider the ERVs obtained in the mid-latitude region ±(20°–52°) and dominating the post-midnight (morning) sector. It is well seen that their variations P_{ERV} have no obvious dependence on the *Kr*-index when the latter is delayed by 3-6 hours. However, when *Kr*-index is delayed by 9 hours, P_{ERV} values are in direct dependence on *Kr*: when *Kr* increases, P_{ERV} values show a slight increase (Fig. 3*c*).

As indicated earlier, a similar result was obtained from DE 2 satellite data [Palmroth et al., 2000]. A direct correlation of P_{EPB} and *Kr*-index values was revealed for the morning EPB cases (23-06 MLT) (Fig. 10 in [Palmroth et al., 2000]). Moreover, the best correlation occurred with *Kr*-index delayed for 2-4 hours and 9 hours. The results obtained by us and Palmroth et al. [2000] results echoed only at a *Kr*-index delay of 9 hours. Apparently, the peculiarities of the orbital parameters of the ISS-b (~972-1220 km, 1978-1979) and DE 2 (~309-1012 km, 1981-1983) satellites, their instrumental difference, and the difference in the level of solar activity and duration of observations make their corrections to the compared results.

What electrodynamic processes are responsible for the response of the probability of observations of postmidnight EPWs to the development of geomagnetic disturbances?

It is known that the IDD electric fields in the post-midnight period change their polarity from western to eastern. In this case, the most favorable conditions for the formation of ESF (ESF) occur after a significant and sudden decrease of convection at high latitudes, when the fast penetration fields (PP) and perturbed IDD electric fields lead to the development of a significant nocturnal upward plasma drift with the largest amplitude at~ 04:00 LT [Fejer et al., 1999]. (It should be mentioned that these conclusions are drawn when analyzing radar data obtained in obs. The significant upward plasma drift appearing in the post-midnight period as a response to the influence of IDD and PP fields is a perturbed (induced) drift in contrast to the downward drift regular for this time. The perturbed drift raises the F-region to higher altitudes, where the frequency of ion-neutral collisions decreases and the rate of RT-unsteadiness increases, leading to the generation of ERVs. This perturbed drift can easily overcome small downward regular drifts of the quiet period.

It is true that a sudden intensification of convection leads to the development of electric fields (PP) of the western direction, which increases the downward drift velocity, decreases the height of

the *F*-region and prevents the formation of inhomogeneities. Obviously, when considering the *Kr*-index with a small delay (e.g., 3 hours), the processes leading to the appearance of drift of different directionality are still noticeable and are reflected in a sharp rise or fall of P_{EPB} values at close values of *Kr*. In general, the general tendency of P_{EPB} dependence on *Kr*-index is not yet observed. However, when delaying the *Kr*-index for 9 hours, when after several hours of increased geomagnetic activity the IDD mechanism is fully "turned on", a small increase of P_{EPB} values can be seen at the growth of geomagnetic activity. Why small?

According to [Fejer et al., 1999], the relationship of post-midnight ESFs to the anomalous reversal of the regular (ordinary) downward drift to the upward drift may depend on the solar cycle. The perturbed drift can easily overcome the small downward drifts of the quiet period during the epoch of solar minimum. However, under more intense solar activity, a larger perturbed drift is required to form post-midnight ESFs (ESFs) because the downward drift rate increases significantly during solar maximum. Our results obtained from ISS-b satellite data (1978− 79) in years of increased solar activity (*F*10.7~150-220) provide evidence for this: the post-midnight increase in P_{ESF}appears to be small.

c) As it was revealed (Tables 1 and 2; Figs. 2 and 3), EPWs are more frequently recorded at mid-latitudes than at the equator and low latitudes. What can explain this difference?

Briefly, it depends on the ratio between the background concentration of He^+ and the depletion value of the plasma bubble in the concentration of He^+. (Recall that ERVs were defined from ISS-b satellite data as plasma regions with depleted concentration in helium ions of He^+, i.e., detected by fluctuations of a single ion component (see, e.g., [Sidorova, 2021]).) Let us consider this in more detail.

As it is known EPBs are formed at the heights of the base of the *F*-region. It is well known that at these heights helium ions are present in very small amounts. For example, according to radar measurements at Arecibo station [Wilford et al., 2003] during the period of high solar activity (October, 2001) the absolute concentration of He^+ at these heights was ~$3\text{-}10^3$ cm^{-3}. Obviously, as the bubble rises to the heights of the upper ionosphere (ISS-b, ~972-1220 km), it gradually "appears" (becomes "visible") as a structure strongly depleted in He^+ ions. It becomes "visible" as the ambient background concentration of He^+ at these altitudes increases significantly and reaches its maximum values (may even be dominant [Heelis et al., 1990]), which gives a good contrast with the minuscule concentration of He^+ inside the plasma bubble.

However, the bubble will not be equally well visible at all latitudes over which it pops and "stretches". This depends on the latitudinal profile of the background He^+ concentration. The behavior of the latitudinal profile will precisely determine the latitudinal regions with different degrees of "visibility" of the plasma bubble.

In the night hours at the upper ionosphere heights in the background He concentration$^+$ an equatorial dip develops, in the trough and at the crests of which EPBs can be registered. The trough of the equatorial failure itself falls at latitudes ~(±20°), and the crests of the failure can reach ±30°–40° (see, for example, [Taylor, 1971]). EPBs are most clearly visible on the crests of the failure: the top of the ridge, the inner and outer slopes of the ridge. The bubbles can be seen very well because they contrast best with the increased background He^+ concentration here. It is somewhat more difficult to register EPBs in the depression of the failure, because the background He^+ concentration in the depression is much lower and contrasts worse with the He^+ concentration inside the bubble. This explains the significant difference in the probability of observing ERVs at different latitudes. In the trough region of the equatorial failure of the background He^+ concentration, i.e., at latitudes ~(±20°), the probability of observing ERVs is lowered, while at the latitudes of ridges with slopes, i.e., at mid-latitudes ±(20°–52°), ERVs are detected much more frequently.

Thus, we obtained a clear picture of the EPW manifestation at midlatitudes, i.e., those EPWs that dominate in the postmidnight sector. This allows us to confidently conclude that we obtained confirmation of the idea about the influence of the IDD mechanism on the generation of postmidnight EPWs, which "turns on" after several hours of increased geomagnetic activity and favors the generation. However, according to the study, this influence is small in years of increased solar activity, which is consistent with the indications of [Fejer et al., 1999]

5. CONCLUSION

Repeated attempts have been made to investigate the influence of geomagnetic activity on the generation of equatorial plasma bubbles. To date, it is well known that geomagnetic activity tends to suppress the generation and development of EPBs in the pre-midnight sector. As for the post-midnight sector, it is believed [Bowman, 1978; Burke, 1979; Singh et al., 1997] that the probability of observing EPBs after midnight will increase as geomagnetic activity increases. However, there are indications [Fejer et al., 1999] that its growth rates will depend on the level of solar activity. In the minimum of solar activity, they will be the most significant. To confirm these ideas, a sufficient amount of observational data is required. For this purpose, the EPB observations obtained in the pre-midnight and post-midnight sectors aboard the ISS-b satellite (~972-1220 km, August 1978-December 1979) are best suited for this purpose. The data were considered in two latitude regions: equatorial-low-latitude ±20° and mid-latitude ±(20°-52°). For both groups, LT- and *Kr*-variations of the probability of ERV observations were calculated. The analysis allows us to draw the following conclusions.

1. EPWs registered at low and equatorial latitudes have the maximum probability of observation in the pre-midnight sector. The probability of their observation decreases as the *Kr*-index taken 3 and 9 hours before the EPW registration increases.

2. EPWs registered at midlatitudes have the maximum probability of observation in the postmidnight sector. The probability of their observation slightly increases with the increase of the *Kr*-index taken 9 hours before the ERV registration.

REFERENCES

1. *Sidorova L.N., Filippov S.V.* Longitudinal statistics of plasma "bubbles" visible at the altitudes of the upper ionosphere in the concentration of He+ // Geomagnetism and Aeronomy. V. 53. No. 1. P. 64−77. 2013. https://doi.org/10.7868/S0016794012060107

2. *Sidorova L.N.* Equatorial plasma “bubbles”: dependence on local time // Geomagnetism and Aeronomy. V. 60. No. 5. P. 557–565. 2020. https://doi.org/10.31857/S0016794020050144

3. *Sidorova L.N.* Equatorial Plasma “Bubbles”: Variability of Latitudinal Distribution with Height // Geomagnetism and Aeronomy. V. 61. No. 4. P. 445–456. 2021. https://doi.org/10.31857/S0016794021040167

4. *Sidorova L.N.* Equatorial plasma bubbles: influence of thermospheric meridional winds // Geomagnetism and Aeronomy. V. 62. No. 3. P. 374–382. 2022. https://doi.org/10.31857/S0016794022030166

5. *Sidorova L.N.* Probability of observing equatorial plasma bubbles depending on the month of the year // Geomagnetism and Aeronomy. V. 63. No. 2. P. 238–246. 2023a. https://doi.org/10.31857/S0016794022600533

6. *Sidorova L.N.* Equatorial plasma bubbles: influence of zonal thermospheric wind // Geomagnetism and Aeronomy. V. 63. No. 6. P. 798–805. 2023b. https://doi.org/10.31857/S0016794023600369

7. *Basu S., Basu Su., Rich F.J., Groves K.M., MacKenzie E., Coker C., Sahai Y., Fagundes P.R., Becker-Guedes F.* Response of the equatorial ionosphere at dusk to penetration electric fields during intense magnetic storms // J. Geophys. Res. – Space. V. 112. N 8. ID A08308. 2007. https://doi.org/10.1029/2006JA012192

8. *Blanc M., Richmond A.D.* The ionospheric disturbance dynamo // J. Geophys. Res. – Space. V. 85. N 4. P. 1669–1686. 1980. https://doi.org/10.1029/JA085iA04p01669

9. *Bowman G.G.* A relationship between polar magnetic substorms, ionospheric height rises and the occurrence of spread *F* // J. Atmos. Terr. Phys. V. 40. N 6. P. 713–722. 1978. https://doi.org/10.1016/0021-9169(78)90129-0

10. *Burke W.J.* Plasma bubbles near the dawn terminator in the topside ionosphere // Planet. Space Sci. V. 27. N 9. P. 1187−1193. 1979. https://doi.org/10.1016/0032-0633(79)90138-7

11. *Fejer B.G.* Low latitude electrodynamic plasma drifts: A review // J. Atmos. Terr. Phys. V. 53. N 8. P. 677–693. 1991. https://doi.org/10.1016/0021-9169(91)90121-M
12. *Fejer B.G., Scherliess L.* Time dependent response of equatorial electric fields to magnetospheric disturbances // Geophys. Res. Lett. V. 22. N 7. P. 851–854. 1995. https://doi.org/10.1029/95GL00390
13. *Fejer B.G., Scherliess L.* Empirical models of storm time equatorial zonal electric fields // J. Geophys. Res. – Space. V. 102. N 11. P. 24047–24056. 1997. https://doi.org/10.1029/97JA02164
14. *Fejer B.G., Scherliess L., de Paula E.R.* Effects of the vertical plasma drift velocity on the generation and evolution of equatorial spread *F* // J. Geophys. Res. – Space. V. 104. N 9. P. 19859–19869. 1999. https://doi.org/10.1029/1999JA900271
15. *Heelis R.A., Hanson W.B., Bailey G.J.* Distributions of He+ at middle and equatorial latitudes during solar maximum // J. Geophys. Res. – Space. V. 95. N 7. P. 10313−10320. 1990. https://doi.org/10.1029/JA095iA07p10313
16. *Kelley M.C., Fejer B., Gonzales C.* An explanation for anomalous equatorial ionospheric electric fields associated with a northward turning of the interplanetary magnetic field // Geophys. Res. Lett. V. 6. N 4. P. 301–304. 1979. https://doi.org/10.1029/GL006i004p00301
17. *Li G., Ning B., Liu L., Wan W., Liu J.Y.* Effect of magnetic activity on plasma bubbles over equatorial and low-latitude regions in East Asia // Ann. Geophys. V. 27. N 1. P. 303–312. 2009. https://doi.org/10.5194/angeo-27-303-2009
18. *Martinis C.R., Mendillo M.J., Aarons J.* Toward a synthesis of equatorial spread F onset and suppression during geomagnetic storms // J. Geophys. Res. – Space. V. 110. N 7. ID A07306. 2005. https://doi.org/10.1029/2003JA0101362
19. *Palmroth M., Laakso H., Fejer B.G., Pfaff R.F. Jr.* DE 2 observations of morningside and eveningside plasma density depletions in the equatorial ionosphere // J. Geophys. Res. – Space. V. 105. N 8. P. 18429–18442. 2000. https://doi.org/10.1029/1999JA005090
20. *RRL.* Summary plots of ionospheric parameters obtained from Ionosphere Sounding Satellite-b. Tokyo: Radio Research Laboratories. Ministry of Posts and Telecommunications. V. 1−3. 1983.
21. *RRL.* Summary plots of ionospheric parameters obtained from Ionosphere Sounding Satellite-b. Tokyo: Radio Research Laboratories. Ministry of Posts and Telecommunications. Special Report. V. 4. 1985.
22. *Scherliess L., Fejer B.G.* Storm time dependence of equatorial disturbance dynamo zonal electric fields // J. Geophys. Res. – Space. V. 102. N 11. P. 24037–24046. 1997. https://doi.org/10.1029/97JA02165

23. *Senior C., Blanc M.* On the control of magnetospheric convection by the spatial distribution of ionospheric conductivities // J. Geophys. Res. – Space. V. 89. N 1. P. 261−284. 1984. https://doi.org/10.1029/JA089iA01p00261

24. *Sidorova L.N., Filippov S.V.* Topside ionosphere He^+ density depletions: seasonal/longitudinal occurrence probability // J. Atmos. Sol.-Terr. Phy. V. 86. P. 83–91. 2012. https://doi.org/10.1016/j.jastp.2012.06.013.

25. *Singh S., Bamgboye D.K., McClure J.P., Johnson F.S.* Morphology of equatorial plasma bubbles // J. Geophys. Res. – Space. V. 102. N 9. P. 20019−20029. 1997. https://doi.org/10.1029/97JA01724

26. *Sobral J.H.A., Abdu M.A., Takahashi H., Taylor M.J., de Paula E.R., Zamlutti C.J., de Aquino M.G., Borba G.L.* Ionospheric plasma bubble climatology over Brazil based on 22 years (1977–1998) of 630 nm airglow observations // J. Atmos. Sol.-Terr. Phy. V. 64. N 12−14. P. 1517−1524. 2002. https://doi.org/10.1016/S1364-6826(02)00089-5

27. *Stolle C., Lühr H., Rother M., Balasis G.* Magnetic signatures of equatorial spread *F* as observed by the CHAMP satellite // J. Geophys. Res. – Space. V. 111. N 2. ID A02304. https://doi.org/10.1029/2005JA011184. 2006.

28. *Taylor H.A.* Evidence of solar geomagnetic seasonal control of the topside ionosphere // Planet. Space Sci. V. 19. N 1. P. 77–93. 1971. https://doi.org/10.1016/0032-0633(71)90068-7

29. *Watanabe S., Oya H.* Occurrence characteristics of low latitude ionospheric irregularities observed by impedance probe on board the Hinotori satellite // J. Geomagn. Geoelectr. V. 38. N 2. P. 125−131. 1986. https://doi.org/10.5636/jgg.38.125

30. *Wilford C.R., Moffett R.J., Rees J.M., Bailey G.J., Gonzalez S.A.* Comparison of the He+ layer observed over Arecibo during solar maximum and solar minimum with CTIP model results // J. Geophys. Res. – Space. V. 108. N 12. P. 1452−1461. 2003. https://doi.org/10.1029/2003JA009940.

31. *Woodman R.F., La Hoz C.* Radar observations of *F*-region equatorial irregularities // J. Geophys. Res. V. 81. N 31. P. 5447−5466. 1976. https://doi.org/10.1029/JA081i031p05447

Table 1. Numerical characteristics of P_{EPB} variations as a function of the interval value of the *Kr*-index. Equator and low latitude region: ±20°

Kr intervals	*Kr* -INDEX DELAY FOR 3 HOURS		*Kr* -INDEX DELAY FOR 6 HOURS		*Kr* -INDEX DELAY FOR 9 HOURS	
	Number ERUs and spans	P_{EPB}[1], %	Number EPO and spans	P_{EPB}[1], %	Number of EPO and spans	P_{EPB}[1], %
0-1	83 (221)	38	84 (218)	39	93 (223)	41
1^{+} -2	83 (234)	35	101 (255)	40	87 (250)	35
2 -3^{+}	83 (259)	32	82 (263)	31	85 (254)	33
3 -4^{+}	46 (155)	30	43 (172)	25	46 (175)	26
4 -9^{+}	35 (114)	31	31 (100)	31	25 (101)	24

Note: [1]P_{ERV} values are rounded to whole numbers.

Table 2. Numerical characteristics of P_{EPB} variations depending on the interval value of the *Kp*-index. Mid-latitude region: ±(20°-52°)

Kp intervals	CR-INDEX DELAY FOR 3 HOURS		*Kp -INDEX* DELAY FOR 6 HOURS		*Kp -INDEX* DELAY FOR 9 HOURS	
	Number ERUs and spans	P_{EPB}[1], %	Number EPO and spans	P_{EPB}[1], %	Number of EPO and spans	P_{EPB}[1], %
0-1	267 (450)	59	246 (411)	60	251 (444)	56
1^{+} -2	287 (447)	64	317 (517)	61	291 (490)	59
2 -3^{+}	317 (555)	57	311 (525)	59	315 (537)	59
3 -4^{+}	206 (341)	60	211 (369)	57	214 (361)	59
4 -9^{+}	151 (244)	62	136 (217)	63	138 (218)	63

Note: [1]P_{ERI}values are rounded to whole numbers.

FIGURE CAPTIONS

Fig. 1. LT variations of the EPB observation probability (P_{EPB}).
(*a*) - Equator and low latitude region: ±20°.
(*b*) - Mid-latitude region: ±(20°-52°).

Fig. 2. Variations of P_{EPB} as a function of the interval value of the *Kr*-index. Equator and low latitude region: ±20°.
(*a*) - Delay of the *Kr*-index for 3 hours
(*b*) - *Kr* -index delay of 6 hours
(*c*) - *Kr* -index delay for 9 hours.

Fig. 3. Variations of P_{EPB} as a function of the interval value of the *Kr*-index. Mid-latitude region: ±(20°-52°).
(*a*) - *Kr* -index delayed for 3 hours
(*b*) - *Kr* -index delayed for 6 hours
(*c*) - Delay of *Kr* -index for 9 hours

Fig. 4. Schematic representation of the evolution of equatorial plasma bubbles with respect to magnetic force tubes, dipole latitude, and altitude. Horizontal lines show the approximate flyby altitudes of the ISS-b (~972-1220 km), ROCSAT-1 (~600 km), and AE-E (~350– 475 km) satellites.

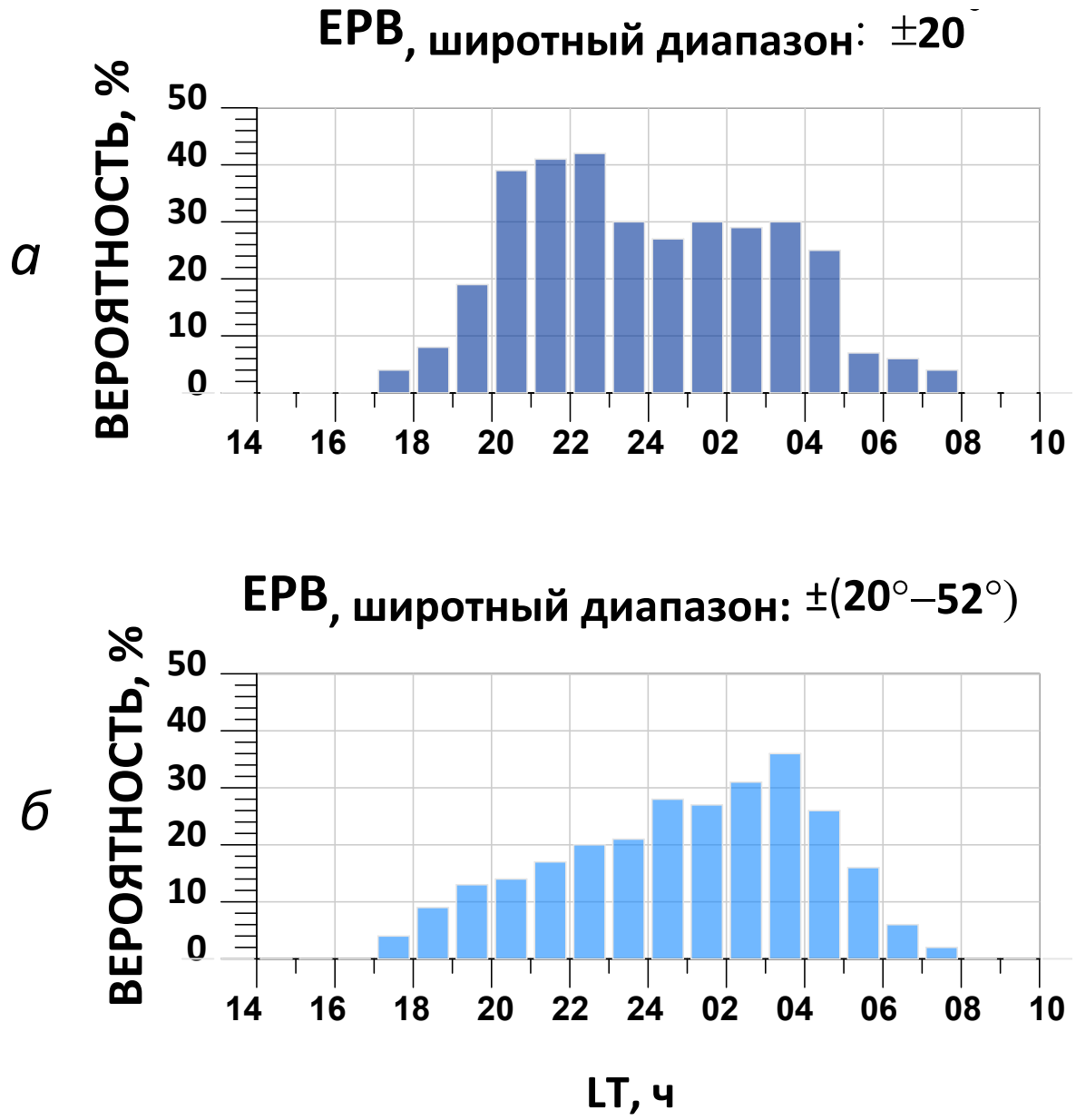
а
EPB, широтный диапазон: ±20°
ВЕРОЯТНОСТЬ, %
50
40
30
20
10
0
14
16
18
20
22
24
02
04
06
08
10
б
EPB, широтный диапазон: ±(20°–52°)
ВЕРОЯТНОСТЬ, %
50
40
30
20
10
0
14
16
18
20
22
24
02
04
06
08
10
LT, ч

Fig. 1.

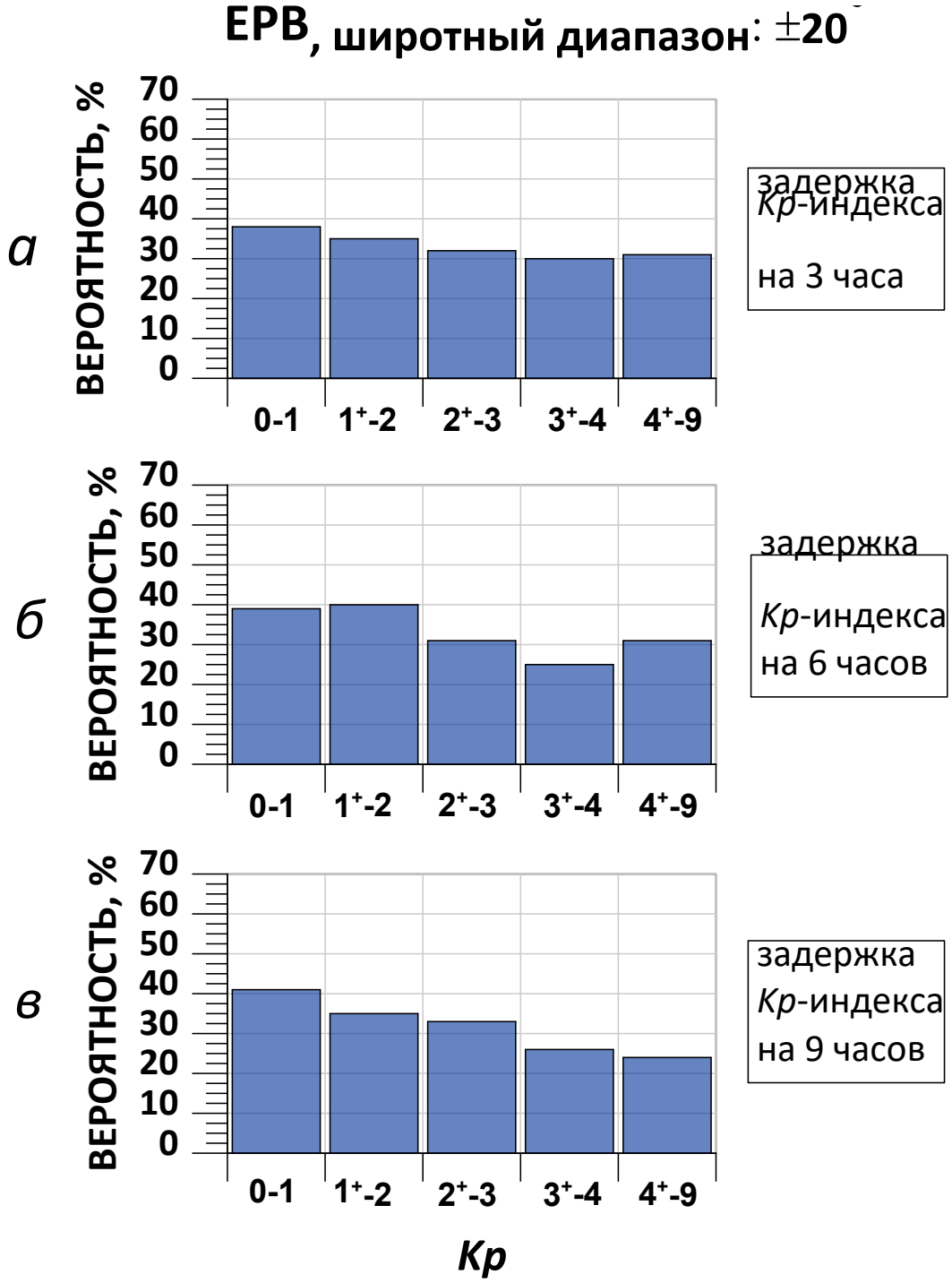
EPB, широтный диапазон: ±20°
а
б
в
ВЕРОЯТНОСТЬ, %
70
60
50
40
30
20
10
0
0-1
1+-2
2+-3
3+-4
4+-9
Kp
задержка Kp-индекса на 3 часа
задержка Kp-индекса на 6 часов
задержка Kp-индекса на 9 часов

Fig. 2.

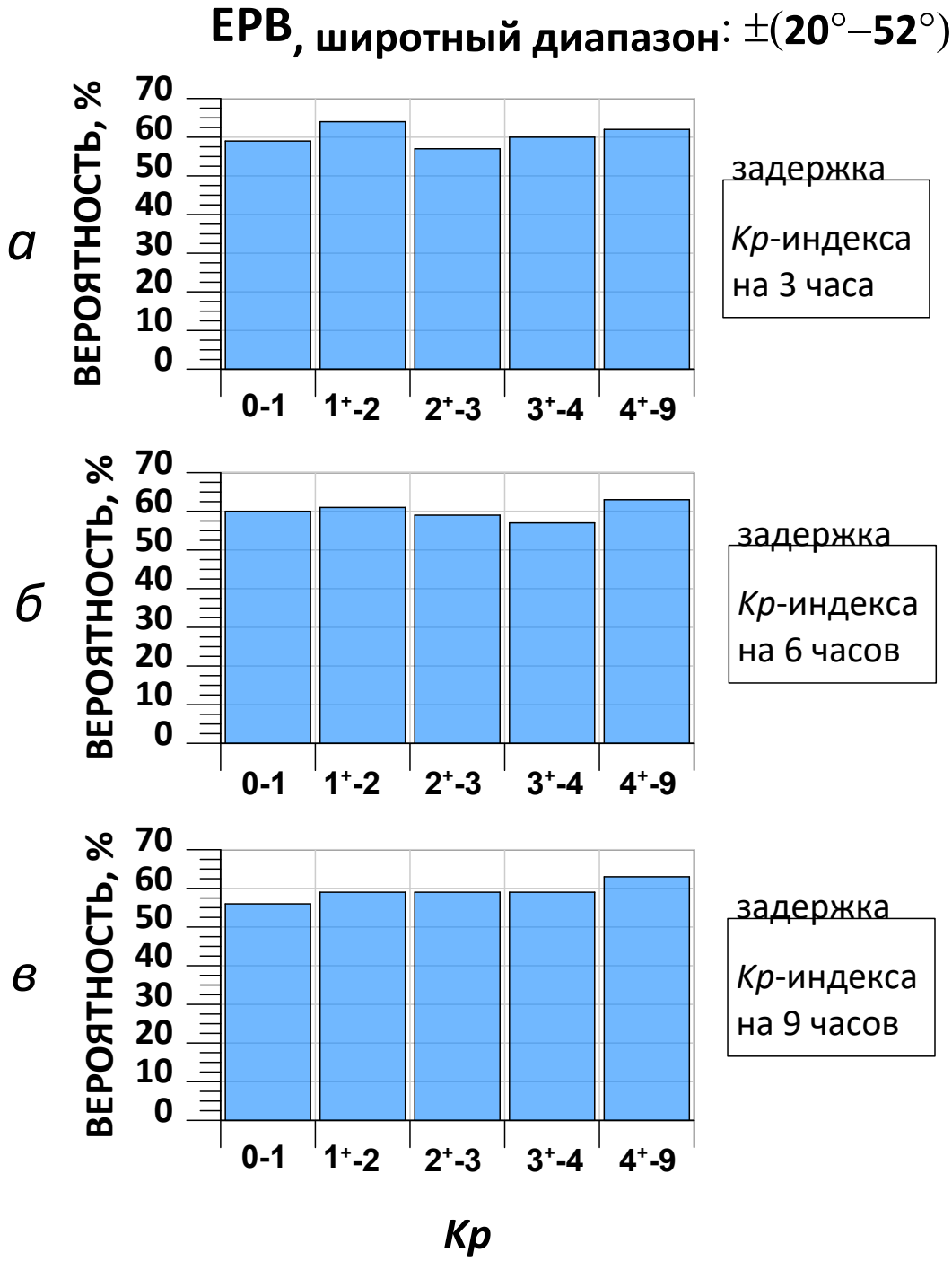
EPB, широтный диапазон: ±(20°–52°)
а
б
в
ВЕРОЯТНОСТЬ, %
70
60
50
40
30
20
10
0
0-1
1+-2
2+-3
3+-4
4+-9
Kp
задержка
Kp-индекса
на 3 часа
задержка
Kp-индекса
на 6 часов
задержка
Kp-индекса
на 9 часов

Fig. 3.

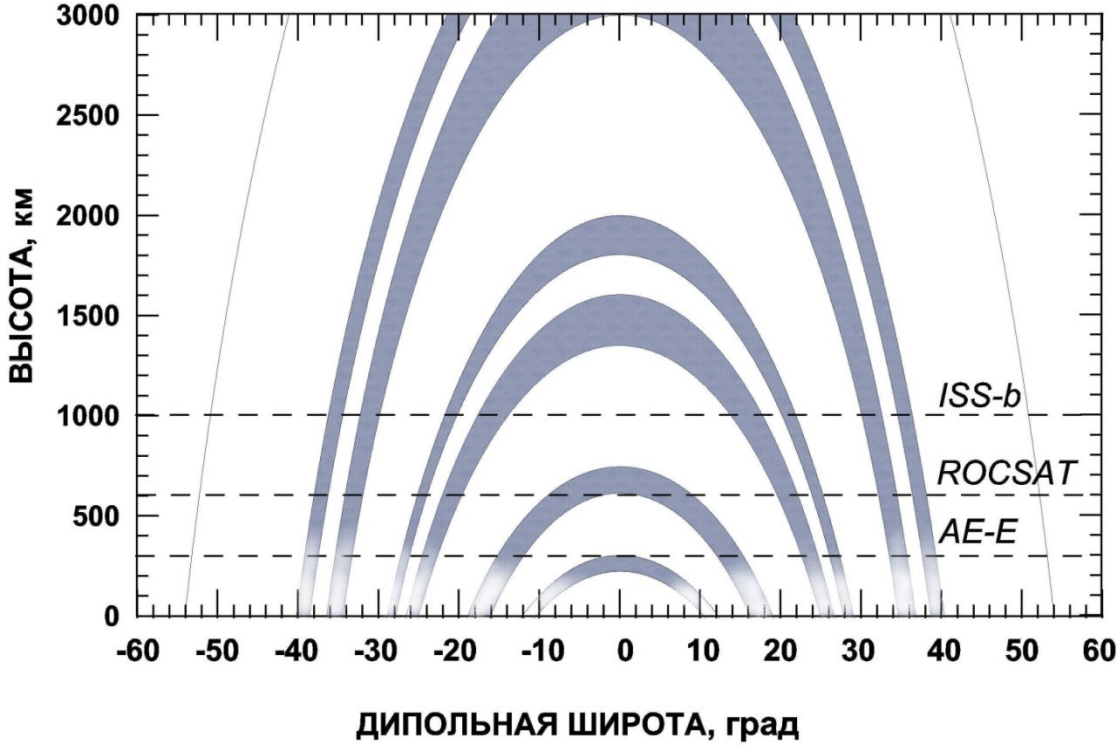
3000
2500
2000
1500
1000
500
0
ВЫСОТА, км
ISS-b
ROCSAT
AE-E
-60
-50
-40
-30
-20
-10
0
10
20
30
40
50
60
ДИПОЛЬНАЯ ШИРОТА, град

Fig. 4.